Critical behavior of the two- and three-dimensional contact replication processes

S. C. Ferreira, Jr.*
Departamento de Física, Universidade Federal de Viçosa, 36571-000, Viçosa, Minas Gerais, Brazil
(Received 20 August 2004; published 27 January 2005)

The two- and three-dimensional contact replication processes (CRP) for monoclonal reproduction were analyzed through intensive Monte Carlo simulations. In these models, the occupation rates are equally divided among the empty nearest neighbor sites of an occupied site. As the one-dimensional case, the two-dimensional version of the model belongs to the directed percolation universality class and the critical rate defining the absorbing state transition is $\lambda_c = 1.083\,20(7)$. However, the critical exponents of the three-dimensional CRP are those of the four-dimensional original contact process and, consequently, the data suggest that the CRP model has a distinct upper critical dimension $d_c = 3$.

DOI: 10.1103/PhysRevE.71.017104 PACS number(s): 05.70.Ln, 05.65.+b, 02.50.Ey

The counterpart of the Ising model for the nonequilibrium statistical mechanics is the contact process (CP) proposed by Harris [1] as a model of epidemics. In the CP model, particles represented by occupied sites of a regular lattice die at a rate 1 whereas empty sites are occupied at a rate $k\lambda/q$. Here, k is the number of occupied nearest-neighbor (NN) sites of an empty site and q is the coordination number of the lattice. As the ratio of infection and death increases, the system exhibits a critical phase transition from the vacuum to an active state characterized by the directed percolation (DP) universality class [2,3]. The CP critical exponents and rates were precisely determined through series expansions and Monte Carlo simulations in $d=1$, 2, and 3 dimensions [4–9]. Also, the upper critical dimension, in which the critical exponents assume the mean field values, is $d_c = 4$. For a review about contact processes and the DP universality class, see Refs. [10–12].

Due to its importance as a fundamental model, several CP generalizations were proposed [13–20]. All these models preserve the DP universality class. A common feature for all mentioned models is that the flow of the infection is equally divided among all the neighbors of the contaminated individuals. This is a reasonable hypothesis for a model of epidemics, but not adequate for a model of monoclonal replication processes such as those occurring in tumor or bacterial growth [21]. Actually, in these cases it is more realistic to suppose the flow of new cells divided just among the empty neighbors because the new cells should occupy empty sites or sites occupied by normal cells in the case of the tumor growth. Several stochastic models have been proposed to simulate monoclonal cell reproduction [22–26]. The simplest one is the Williams and Bjerknes (WB) model [23], in which death and reproduction are considered only for cells with at least one empty NN site. The WB model does not belong to the DP universality class. Recently, we studied a modified one-dimensional version of the CP, in which cells with at least one empty neighbor site replicate at rate λ but any cell dies at rate 1 [27]. The new cells generated from the division occupy one of their empty NN sites chosen at random. Since only cells in "contact" with empty sites can replicate, we refer to this model as a *contact replication process* (CRP). This model is a hybrid of the CP and the WB models. It was shown through Monte Carlo simulations in $d=1$ that the CRP model belongs to the DP universality class [27].

In the present work, we analyze the contact replication processes (CRP) in two and three dimensions. The central concern of this work is about the maintenance (or not) of the DP universality class in higher dimensions. As we shall demonstrate, in $d=2$ the model belongs to DP class, but in $d=3$ it is not the case. Indeed, the present numerical results suggest that $d_c = 3$ is the upper critical dimension of the model, in which the mean field critical exponents are obtained.

As in the original CP, the cells lie on a regular lattice with periodic boundaries, in which $\sigma_i = 1$ represents an occupied and $\sigma_i = 0$ an empty site. The dynamics of the CRP includes two processes, namely, cell death and reproduction. A cell dies at constant rate 1. In turn, if a cell has at least one empty NN site, it replicates at rate λ and its daughter cell occupies one of its empty NN sites chosen with equal probabilities. Notice the subtle but essential difference between CRP and CP. In CP, an occupied site infects each one of its empty NN sites at rate λ/q independently of their number. In contrast, in the CRP the occupation rates depend on the number of empty NN sites, i.e., an occupied site infects each one of its empty NN sites at rate λ/n^*, where n^* is its number of empty NN sites. If the reproduction rate is not sufficiently large, the vacuum always is reached. The discrete-time formulation of the CRP used in the simulations is the following. At each time step, one occupied site (a cell) is chosen at random. The chosen cell dies with probability $p = 1/(1+\lambda)$. In turn, the cell replicates with probability $1-p$ if at least one of their NN sites is empty. If all the NN sites are occupied, the cell does not replicate. But, if the replication occurs, one of their empty NN sites is occupied with equal probabilities. After each step, the time is incremented by $\Delta t = 1/n$, where n is the number of cells just prior the event.

To determine the CRP critical rate in $d=2$ and 3 dimensions, we considered the CRP starting with a single particle at the origin [10,11]. The behaviors of some time-dependent quantities, namely, the survival probability $P(t)$, the mean number of occupied sites

*Electronic address: silviojr@ufv.br

$$n(t) = \left\langle \sum_{\mathbf{r}} \sigma_{\mathbf{r}}(t) \right\rangle, \tag{1}$$

and the spreading

$$R^2(t) = \frac{1}{n(t)} \left\langle \sum_{\mathbf{r}} r^2 \sigma_{\mathbf{r}}(t) \right\rangle \tag{2}$$

were analyzed. Here $\langle \cdots \rangle$ represents the average over all trials, including those reaching the absorbing configuration before time t, and $\mathbf{r}$ the position of the site measured from the initial seed. In the subcritical regime ($\lambda < \lambda_c$) both $P(t)$ and $n(t)$ decay exponentially, whereas the spreading is diffusive with $R^2(t) \sim t$ if the CRP obeys the usual scaling theory for absorbing phase transitions. In the supercritical regime ($\lambda > \lambda_c$), $P(t)$ reaches a constant and finite value, $n(t) \sim t^d$, and $R^2(t) \sim t^2$, when $t \to \infty$ [11]. Exactly at the critical point ($\lambda = \lambda_c$), these quantities asymptotically follow power laws $P(t) \sim t^{-\delta}$, $n(t) \sim t^{\eta}$, and $R^2(t) \sim t^z$. Notice that z is frequently used in the literature to represent the dynamic exponent, but here z refers to the spreading exponent. For the DP universality class, these exponents obey the hyperscaling relation $4\delta + 2\eta = zd$ for $d \leqslant 4$ [2]. Thus, the double-logarithm plots of these quantities near the critical point exhibit an upward (downward) curvature for $\lambda > \lambda_c$ ($\lambda < \lambda_c$).

In Fig. 1(a), double-logarithm plots of $P(t)$ and $n(t)$ versus time for the two-dimensional CRP and distinct λ values around the critical point are shown. To determine the point of null curvature, the double-logarithm data are fitted by cubic polynomials $P_3(t)$ and the mean curvature is defined as

$$\langle \kappa \rangle = \frac{1}{\log_{10} t_f - \log_{10} t_i} \int_{\log_{10} t_i}^{\log_{10} t_f} \kappa(t), \tag{3}$$

where t_i (t_f) is the initial (final) time used for the fittings and $\kappa(t)$ is the local curvature defined by the usual formula

$$\kappa = \frac{P_3''}{[1 + (P_3')^2]^{3/2}}. \tag{4}$$

We used $t_i = 10^2$ and $t_f = 10^5$ for all λ values. The critical point is determined by extrapolating the data using a quadratic fitting [Fig. 1(b)]. The critical rate obtained considering $P(t)$ was $\lambda_c = 1.083\,20\,33$ and the value obtained using $n(t)$ was $\lambda_c = 1.083\,211\,3$. Thus, $\lambda_c = 1.083\,20(7)$ was adopted, where the number in parentheses reflects the uncertainty. Notice that the CRP critical rate in $d = 2$ is smaller than the correspondent rate of CP $\lambda_c^{CP} = 1.6488(1)$ [10]. Indeed, this is expected since transitions evolving the birth of a new particle occur at rate λ/q in CP and at rate λ/n^* in CRP, where $n^* \leqslant q$. In Fig. 2, the ratios between time-dependent quantities and power laws with the critical exponents of the DP class [$\delta = 0.4505(10)$, $\eta = 0.2295(10)$, and $z = 1.1325(10)$ [5,6]] are shown. All the curves asymptotically reach a constant value demonstrating that the two-dimensional CRP belongs to the DP class. The slow convergence of $P(t)$ is due to finite time corrections to the scaling [10,11]

$$P(t) \sim t^{-\delta}(1 + at^{-\theta} + bt^{-\theta'} + \cdots). \tag{5}$$

As for the one-dimensional CRP, the small changes introduced in CP with CRP are not able to remove the latter contact process from the DP universality class, but its critical rate is significantly altered.

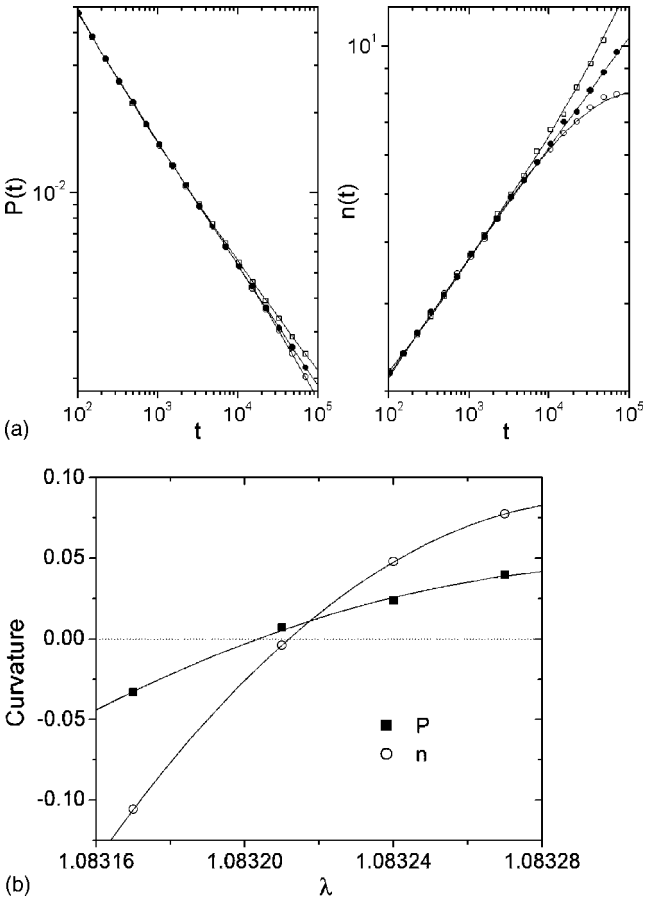

FIG. 1. (a) Survival probability and mean number of particles versus time for the two-dimensional CRP. In these plots, 10^6 samples were used to simulate the rates $\lambda = 1.083\,17$ (open circles), 1.083 21 (filled circles), and 1.083 24 (squares). The solid lines correspond to cubic polynomial fits with coefficient of correlation $r^2 > 0.9999$. (b) Curvature as a function of λ obtained from the cubic fits. The solid lines represent quadratic fits.

Now, we introduce the scaling hypothesis of Grassberger and de la Torre [2] near the critical point

$$P(\Delta, t) \simeq t^{-\delta} f(\Delta t^{1/\nu_\parallel}), \tag{6}$$

where $\nu_\parallel$ is a universal critical exponent and $\Delta = |\lambda - \lambda_c|$. Similar relations are expected for $n(t)$ and $R^2(t)$. In the subcritical regime the survival probability decays exponentially for $t \to \infty$, and consequently the scaling function must assume the form $f(x) \sim x^{\nu_\parallel \delta} \exp(-ax^{\nu_\parallel})$, where a is a positive constant. Introducing $f(x)$ in Eq. (6) we obtain $P \sim \exp(-a\Delta^{\nu_\parallel} t)$ and the characteristic relaxation time diverges as $\xi_\parallel \sim \Delta^{-\nu_\parallel}$. $\xi_\parallel$ can be obtained from the linear regression of $\ln(P)$ or $\ln(n)$ as a function of t for long times.

In Fig. 3(a), two examples of the $\xi_\parallel$ determination are shown. The number of independent runs and time steps used to generate these curves varied from 10^8 and 10^2 for the larger Δ values, respectively, to 10^6 samples with 10^5 time steps for the smaller ones. In Fig. 3(b), the characteristic time $\xi_\parallel$ determined through the $\ln(n)$ versus t curves is plotted as

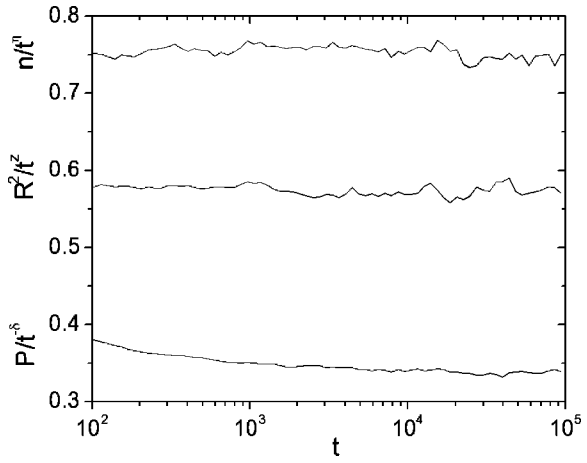

FIG. 2. Ratios between the time-dependent quantities for CRP at $\lambda = 1.083\,21$ and the correspondent power laws of the DP universality class. In these simulations, 10^6 independent trials were used.

a function of the distance from the critical point Δ. The slope of the line is $\nu_\parallel = 1.2907$ while the slope obtained using the curves $\ln(P)$ versus t is $\nu_\parallel = 1.2762$. Thus, $\nu_\parallel = 1.28(3)$ was adopted. This exponent value is in good agreement with the

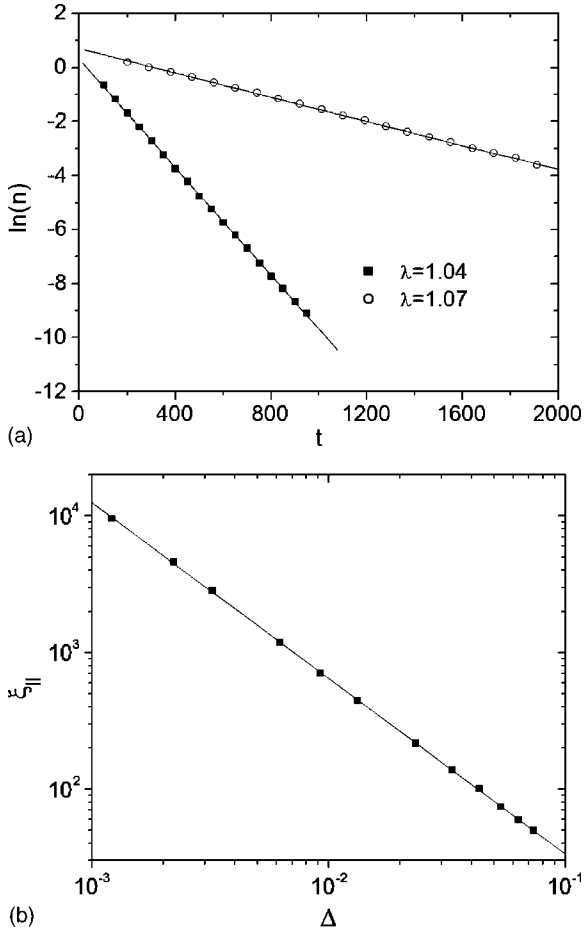

FIG. 3. Determination of the critical exponent $\nu_\parallel$. (a) Examples of the exponential decays observed for the subcritical regime. (b) Characteristic time $\xi_\parallel$ as a function of the distance from the critical point Δ.

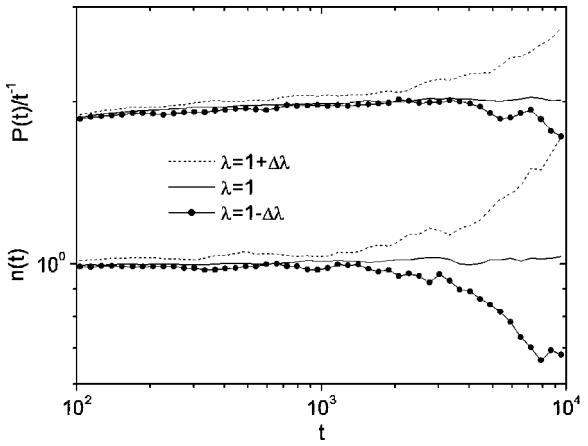

FIG. 4. The ratios between the time-dependent quantities and the corresponding power laws for the three-dimensional CRP. The deviation from unity is $\Delta\lambda = 10^{-4}$ and the averages were done over 10^6 independent trials.

CP exponent $\nu_{\parallel_{CP}} = 1.295(6)$ [6]. Other exponents are defined in the DP class, but they depend on the previously determined exponents [10]. Near the critical point, the stationary density $\rho \sim \Delta^\beta$, the correlation length $\xi_\perp \sim \Delta^{-\nu_\perp}$, and the variance of stationary density $\chi \sim \Delta^{-\gamma}$ define the remaining critical exponents that obey the relations $\beta = \delta\nu_\parallel$, $2\nu_\perp = z\nu_\parallel$, and $\gamma = d\nu_\perp - 2\beta$ [10].

Simulations of CRP in the cubic lattice provide a critical rate $\lambda_c \simeq 1$. The critical exponents are very close to those of the four-dimensional CP, i.e., $\delta = 1$, $\eta = 0$, and $z = 1$ [10]. In Fig. 4, P/t^{-1} and n versus time are plotted for critical, subcritical, and supercritical λ values. For $\lambda \equiv 1$ the curves are nearly time independent, but a small perturbation ($\Delta\lambda = 10^{-4}$) in the rate $\lambda = 1$ clearly causes an upward ($\lambda > \lambda_c$) or downward ($\lambda < \lambda_c$) deviation from the constant. However, a critical rate larger than unity is expected for any finite d. So, in the present case, the λ_c value is so close to unity (in agreement with our simulations the difference is lower than 10^{-5}) that the difference cannot be observed within our cur-

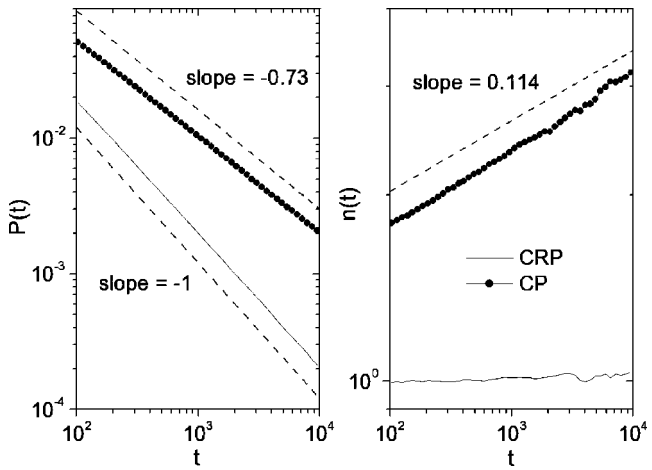

FIG. 5. Comparisons between three-dimensional CP and CRP at the critical points $\lambda_c = 1.3169(1)$ [10] and $\lambda_c = 1$, respectively. 10^6 independent trials were used in these simulations.

rent numerical uncertainties. This result is somewhat unexpected since small alterations in the CP generally do not change the DP class [14–17]. Indeed, even significant alterations, as for example the inclusion of new absorbing configurations, can affect dynamic exponents but the static exponents of CP are preserved [18–20,28–30]. These results suggest that the CRP has a different upper critical dimension of the CP. This change probably occurs due to the next-nearest-neighbor dependence in the replication rates, which becomes more significant as the lattice coordination number is increased.

The clear difference between three-dimensional CRP and CP is illustrated in Fig. 5, in which the time-dependent quantities P and n for CRP and CP are compared. Also, the respective power laws for the DP class in $d=3$ [$\delta=0.730(4)$ and $\eta=0.114(4)$ [7]] and $d=4$ ($\delta=1$ and $\eta=0$) are indicated by the dashed lines. Finally, $\nu_{\|}$ was determined and the mean field value $\nu_{\|}=1$ was obtained.

In summary, the contact replication process in two and three dimensions was studied through intensive Monte Carlo simulations. The two-dimensional model belongs to the directed percolation universality class with a critical rate defining the absorbing state transition $\lambda_c=1.083\,20(7)$. However, the three-dimensional CRP exhibits the mean field critical exponents indicating that the upper critical dimension of the model is $d_c=3$, in contrast to the conventional contact process for which $d_c=4$. This fact illustrates how important are the details of the biological modeling rules. In particular, this work suggests that an epidemic can be equivalent to a reproduction process in low-dimensional systems, but not in three-dimensional ones. A potential application for these models (CP and CRP) is tumor virotherapy modeling [31], in which viruses that replicate selectively in cancer cells can kill them. In this reaction-diffusion model, a CP-like model will govern the virus dynamics while CRP will determine the tumor cells dynamics.

I thank M. L. Martins and J. A. Redinz for the critical reading of this manuscript. This work was supported by CNPq, a Brazilian agency.

[1] T. E. Harris, Ann. Prob. **2**, 969 (1974).
[2] P. Grassberger and A. de la Torre, Ann. Phys. (N.Y.) **122**, 373 (1979).
[3] R. Dickman and I. Jensen, Phys. Rev. Lett. **67**, 2391 (1993); I. Jensen and R. Dickman, J. Stat. Phys. **71**, 89 (1993).
[4] I. Jensen, J. Phys. A **32**, 5233 (1999).
[5] C. A. Voigt and R. M. Ziff, Phys. Rev. E **56**, R6241 (1997).
[6] P. Grassberger and Y.-C. Zhang, Physica A **224**, 169 (1996).
[7] I. Jensen, Phys. Rev. A **45**, R563 (1992).
[8] R. Dickman, Phys. Rev. E **60**, R2441 (1999).
[9] S. M. Dammer and H. Hinrichsen, J. Stat. Mech.: Theory Exp. **1**, P07011 (2004).
[10] J. Marro and R. Dickman, *Nonequilibrium Phase Transitions in Lattice Models* (Cambridge University Press, Cambridge, U.K., 1999).
[11] R. Dickman, in *Nonequilibrium Statistical Mechanics in One Dimension* (Cambridge University Press, Cambridge, U.K., 1999).
[12] H. Hinrichsen, Adv. Phys. **49**, 815 (2000).
[13] R. Durret and D. Griffeath, Ann. Prob. **11**, 1 (1983).
[14] M. Katori and N. Konno, Physica A **186**, 578 (1992).
[15] T. Tomé and M. J. de Oliveira, Phys. Rev. Lett. **86**, 5643 (2001).
[16] R. Dickman and T. Tomé, Phys. Rev. A **44**, 4833 (1991).
[17] R. Dickman, Phys. Rev. B **40**, 7005 (1989).
[18] I. Jensen, Phys. Rev. Lett. **70**, 1465 (1993).
[19] I. Jensen and R. Dickman, Phys. Rev. E **48**, 1710 (1993).
[20] R. Dickman, W. R. M. Rabêlo, and G. Ódor, Phys. Rev. E **65**, 016118 (2001).
[21] R. A. Weinberg, Sci. Am. **275**(3), 62 (1996).
[22] M. Eden, in *Proceedings of Fourth Berkeley Symposium on Mathematical Statistics and Probability, Vol. IV: Biology and Problems of Health*, edited by J. Neyman (University of California Press, Berkeley, 1961), p. 223.
[23] T. Williams and R. Bjerknes, Nature (London) **236**, 19 (1972).
[24] D. Drasdo, R. Kree, and J. S. McCaskill, Phys. Rev. E **52**, 6635 (1995).
[25] Y. Louzoun, S. Solomon, H. Atlan, and I. R. Cohen, Bull. Math. Biol. **65**, 375 (2003).
[26] S. C. Ferreira, Jr., Physica A **317**, 565 (2003).
[27] S. C. Ferreira, Jr., Phys. Rev. E **70**, 036119 (2004).
[28] J. K. L. da Silva and R. Dickman, Phys. Rev. E **60**, 5126 (1999).
[29] C. López and M. A. Muñoz, Phys. Rev. E **56**, 4864 (1997).
[30] G. Ódor, J. F. F. Mendez, M. A. Santos, and M. C. Marques, Phys. Rev. E **58**, 7020 (1998).
[31] S. C. Ferreira, Jr., M. L. Martins, and M. J. Vilela, Physica A **345**, 591 (2005).